HOKKAIDO UNIVERSITY

Title	Extramammary Paget's disease patient-derived xenografts harboring ERBB2 S310F mutation show sensitivity to HER2-targeted therapies
Author(s)	Maeda, Takuya; Kitamura, Shinya; Nishihara, Hiroshi; Yanagi, Teruki
Citation	Oncogene, 39, 5867-5875 https://doi.org/10.1038/s41388-020-01404-x
Issue Date	2020-09-03
Doc URL	http://hdl.handle.net/2115/80541
Type	article (author version)
Additional Information	There are other files related to this item in HUSCAP. Check the above URL.
File Information	Oncogene_39_5867.pdf

Instructions for use

2   **Extramammary Paget's disease patient-derived xenografts harboring ERBB2**

3   **S310F mutation show sensitivity to HER2-targeted therapies**

4   Takuya Maeda[1][¶], Shinya Kitamura[1][¶], Hiroshi Nishihara[2], Teruki Yanagi[1][*]

5   [1] *Department of Dermatology, Faculty of Medicine and Graduate School of Medicine,*

6   *Hokkaido University, Sapporo, Japan*

7   [2] *Genomics Unit, Keio Cancer Center, Keio University School of Medicine, Tokyo,*

8   *Japan*

9

10   *Correspondence to Teruki Yanagi, M.D., Ph.D.

11   *Department of Dermatology, Faculty of Medicine and Graduate School of Medicine,*

12   *Hokkaido University, N15 W7, Kita-ku, Sapporo 060-8638, Japan*

13   Telephone: +81-11-706-7387

14   Facsimile: +81-11-706-7820

15   E-mail: yanagi@med.hokudai.ac.jp

16

17   [¶] These authors contributed equally to this work.

18

19   Word count: 200-word abstract, 2899-word text

20   References: 39

21   Tables: 0

22   Figures: 5

23   Supplementary figures: 7

24   Supplementary tables: 2

25

26   Running title: A novel experiment model for extramammary Paget's disease

27

28   Abbreviations:

29   EMPD: extramammary Paget's disease

30   G: generation

31   HE: hematoxylin and eosin

32   LOH: loss of heterozygosity

33   PDX: patient-derived xenograft

34   TUNEL: terminal deoxynucleotidyl transferase dUTP nick end labeling

35   VAF: variant allele frequency

36

37

38 **Abstract**

39 Although the prognosis of advanced extramammary Paget's disease (EMPD) is poor,

40 there have been no preclinical research models for the development of novel

41 therapeutics. This study aims to establish a preclinical research model for EMPD. We

42 transplanted EMPD tissue into immunodeficient NOD/Scid mice. Histopathological and

43 genetic analyses using a comprehensive cancer panel were performed. For *in vivo*

44 preclinical treatments, trastuzumab, lapatinib, docetaxel, or eribulin were administered

45 to patient-derived xenograft (PDX) models. Tissue transplanted from the EMPD patient

46 was enlarged in NOD/Scid mice and was transplanted into further generations. Both the

47 transplantation of PDX into *nu/nu* mice and the reanimation of the cryopreserved

48 xenografted tumors in NOD/Scid mice were successful. We also established an EMPD-

49 PDX-derived primary cell culture. Histopathologically, the xenografted tumors were

50 positive for CK7, which was consistent with the patient's tumors. Genetically, the

51 pathogenic mutation *ERBB2* S310F was detected in the patient's tumors (primary

52 intraepidermal lesion, metastatic lymph node) and was observed in the xenografted

53 tumors even after continued passages. The xenografted tumors responded well to

54 trastuzumab and lapatinib therapy. Also, cytotoxic agents (docetaxel and eribulin) were

55 effective against the xenografted tumors. This PDX model (EMPD-PDX-H1) could be a

56 powerful tool for the research and development of EMPD treatments.

3

Introduction

Paget's disease is a rare adnexal neoplasm that was first described by Sir James Paget in

1874 (ref. 1). Extramammary Paget's disease (EMPD) is a variant that is commonly

seen in the genital areas and anus among the senior population (ref. 2), and the number

of cases has been increasing in recent years (ref. 3). In most EMPD cases, tumor cells

are localized in the epidermis, and the prognosis is relatively favourable (ref. 4).

However, once tumor cells invade the dermis, patients are at a risk of lymph node and

visceral metastases, and the prognosis becomes significantly poorer (ref. 5-7). A multi-

center retrospective study by Ohara et al. showed that the 5-year survival rate for EMPD

patients with distant metastasis was only 7% (ref. 7). There have been several

retrospective studies on treatments for metastatic EMPD, such as cytotoxic

chemotherapies (ref. 8-12), and small molecular inhibitors (ref. 13-15). However, the

efficacies of these treatments have been evaluated only in single case reports or case

series containing small numbers of patients. Thus, the development of novel therapeutic

strategy for advanced EMPD has been desired.

In recent years, the usefulness of patient-derived xenograft (PDX) models has

been reported in many types of cancers (ref. 16-18). PDX models have demonstrated an

ability to maintain the characteristics of the original tumor and to be useful for

preclinical therapeutic studies in certain cancers. These models have shown to be

4

76   predictive of clinical outcomes and are being used for preclinical drug evaluation,

77   biomarker identification, biological studies, and personalized medicine strategies (ref.

78   17). For EMPD, Nishi et al. reported the first PDX model using an EMPD tumor in

79   1992 (ref. 19). They transplanted metastatic EMPD tissue into nude mice (*nu/nu* mice).

80   Reportedly, their xenografted tumor maintained the histopathological features of the

81   patient's original tumor, and they investigated the effect of hormonal stimulation on

82   tumor growth. To the best of our knowledge, no additional studies using this PDX

83   model have been published. Thus, no preclinical research models of EMPD including

84   cell lines and PDX are currently available.

85   Here, we report a novel PDX model of EMPD (EMPD-PDX-H1) harboring a

86   pathogenic *ERBB2* mutation. We performed histopathological and genetic analyses to

87   confirm that the xenografted tumors maintained the characteristics of the patient's

88   original tumors. Further, we performed treatment experiments using cytotoxic agents

89   and HER2-targeted therapies.

90   **Results**

91   **Establishment of the EMPD-PDX-H1**

92   A schematic of the present study is shown in Figure 1. To establish a patient-derived

93   EMPD xenograft, surgically resected tissue was transplanted onto the flanks of

94   NOD/Scid mice (Figure 2 A, B). The transplanted EMPD tumor tissue grew into a firm

95   nodule of more than 10 mm in diameter over the course of 5 months (generation 0: G0,

96   Figure 2C). The xenograft tissue was analyzed by HE staining and

97   immunohistochemistry for CK7 and HER2, and for androgen, estrogen and

98   progesterone receptors. The EMPD-PDX-H1 tissue exhibited similar morphology and

99   protein expressions to those of the patient's tissues (primary tumor and metastatic

100   lymph node) (Figure 2D and Supplementary Figure S1). Once the tumor volume

101   reached 500–1000 mm^3, the EMPD-PDX-H1 tumors were transplanted into the next

102   generation of NOD/Scid mice. By the third passage, the growth volume curve of PDX

103   in each generation became stable (Supplementary Figure S2). Also, we transplanted

104   EMPD-PDX-H1 tumors into *nu/nu* mice. Both the transplantation of EMPD-PDX-H1

105   tumors into the *nu/nu* mice (3/3, 100%) and the reanimation of the cryopreserved

106   EMPD-PDX-H1 tumors in the NOD/Scid mice (10/12, 83.3 %) were successful

107   (Supplementary Figure S3 and S4). Also, we established primary culture cells from the

108   3rd generation of EMPD-PDX-H1, in which cultured tumor cells were round or cuboidal

6

109   (Supplementary Figure S5).

110

111   **EMPD-PDX-H1 harbors an *ERBB2* S310F mutation identical to that of the**

112   **patient's tumors**

113   To investigate the characteristics of EMPD-PDX-H1 and the similarity between the

114   patient's tissues (primary tumor and metastatic lymph node) and EMPD-PDX-H1, we

115   performed gene mutation analysis. To compare the cancer-associated genomic profile of

116   the patient's tumors to those of their corresponding xenografts, we performed deep

117   sequencing using a comprehensive cancer panel. EMPD-PDX-H1 tumors faithfully

118   maintained the pathogenic genomic DNA alterations of *ERBB2* (c.929C>T, p.S310F),

119   which was observed in the corresponding tumor (metastatic lymph node) of the patient

120   (Figure 3A). *ERBB2* S310F mutation was conserved even after continued passages of

121   EMPD-PDX-H1 (Figure 3A, PDX (G2)). Sanger sequencing targeting *ERBB2* mutation

122   revealed that the patient's primary tumor (resected 12 years earlier) harbored the

123   identical *ERBB2* S310F mutation (Figure 3B).

124   In addition to *ERBB2* S310F being retained in EMPD-PDX-H1, so were *TP53*

125   A161T and *RB1* S780*. In the patient's lymph nodes, the variant allele frequency (VAF)

126   for *TP53* A161T was 50.4% and for *RB1* S780* was 42.5%. The VAF of both mutations

127   in EMPD-PDX-H1 was elevated to 100% (Supplementary Table S1). This is because

128   the normal allele was lost and the proportion of normal cells decreased in EMPD-PDX-

129   H1 tumor. The mutation of *NF1* D2545N was also retained in EMPD-PDX-H1;

130   however, its VAFs (47.5% in G1 and 50.3% in G2) suggest that the normal allele was

131   sustained. *NOTCH1* S1409N has been observed in EMPD-PDX-H1 tumors (G1 and

132   G2) with high VAF, possibly due to the loss of heterozygosity (LOH). Since no such

133   mutation was detected in the patient's tumor, it might be crucial for PDX implantation.

134

135   **Treatment experiments using EMPD-PDX-H1**

136   Preclinical studies for EMPD have not been reported until this paper, possibly due to the

137   unavailability of EMPD cell lines/PDX tissues. We performed treatment experiments to

138   investigate whether EMPD-PDX-H1 responds to targeted therapies and chemotherapies

139   as reported in clinical settings (Ref. 8-15). For the targeted therapy, since the PDX

140   harbored pathogenic *ERBB2* S310F, we treated the tumor with HER2-targeted therapies

141   (trastuzumab, lapatinib, and combination of the two). The single use of trastuzumab or

142   lapatinib was found to suppress tumor progression, but the combined therapy was found

143   to remarkably inhibit tumor growth (Figure 4, A–F). Regarding cytotoxic

144   chemotherapies, the xenografted model responded well to docetaxel (Figure 5, A, B),

145   which is reported to be effective against metastatic EMPD (Ref. 10, 11). We tested

146   eribulin monotherapy, which has been shown to be effective as a second-line treatment

8

147   for breast cancer (ref. 20). Eribulin therapies (1.5 mg/kg/week) eliminated EMPD-PDX-

148   H1 completely, and no relapse was observed for one week (Figure 5 C, D). We

149   administered 0.45 mg/kg/week eribulin and obtained similar results (Figure 5 E, F). The

150   results of treatment experiments were also confirmed by Ki-67 staining and terminal

151   deoxynucleotidyl transferase dUTP nick end labeling (TUNEL) assays. In Ki-67

152   staining, all of the treated EMPD-PDX-H1 tumors showed a significantly lower ratio of

153   positive cells than the non-treated tumors showed (Supplementary Figure S6). In the

154   TUNEL assays, all of the treated EMPD-PDX-H1 tumors showed a significantly higher

155   ratio of TUNEL-positive tumor cells than the control tumor cells showed

156   (Supplementary Figure S7).

157

158 **Discussion**

159 The present study presented an EMPD PDX model that reproduced the patient's original

160 tumor morphologically and genetically. We also reported the promising potency of

161 HER-2 targeted therapies and cytotoxic chemotherapies.

162   It has been reported that certain EMPD cases revealed overexpression of HER2

163 as assessed by immunohistochemistry and *in situ* hybridization (ref. 21-23). In addition,

164 somatic mutations analyses of EMPD have detected *ERBB2* mutations (ref. 24, 25).

165 Overexpression of HER2 protein and *ERBB2* gene amplification positively correlate

166 with disease progression (ref. 22). Clinically, several case reports have shown the

167 efficacy of HER2-targeted therapies such as lapatinib and trastuzumab against

168 metastatic EMPD (ref.13-15). In light of these facts, the HER2 signalling pathway is

169 considered to contribute to carcinogenesis in HER2-positive/mutated EMPD. In the

170 present study, the PDX model was found to harbor a pathogenic *ERBB2* mutation

171 (S310F) without definitive amplification. *ERBB2* S310F mutation corresponds to the

172 extracellular domain of ERBB2/HER2, and that domain has been reported as having the

173 most common mutation of *ERBB2* in various cancers such as breast, lung, bladder, and

174 colon (ref. 26). Greulich et al. reported that *ERBB2* S310F mutation leads to

175 ERBB2/HER2 activation via two distinct mechanisms, characterized by elevated C-

176 terminal tail phosphorylation or by covalent dimerization through intermolecular

10

177 disulfide bond formation (ref. 27). The S310F mutation has been reported in *ERBB2*

178 non-amplified breast cancer and is not necessarily accompanied by *ERBB2*

179 amplification (ref. 28). Also, HER2-targeted therapy is effective against lung, colon, and

180 other cancers harboring the S310F mutation (ref. 27, 29, 30). Concerning EMPD,

181 Mishra et al. were the first to report a case of EMPD harboring the *ERBB2* S310F

182 mutation in which trastuzumab and capecitabine combination therapy was remarkably

183 effective against multiple metastatic lesions (ref. 15). This case report is consistent with

184 our experimental results showing that EMPD-PDX-H1 harboring *ERBB2* S310F is

185 sensitive to HER2-targeted therapies. In addition, a phase 2 clinical study using

186 trastuzumab combined with docetaxel for HER2-positive EMPD (UMIN000021311) is

187 under way at Keio University in Japan.

188   The present study has also demonstrated the antitumor effects of cytotoxic

189 chemotherapies. We herein tried the administration of eribulin, an inhibitor of

190 microtubule dynamics that has proven effective against breast cancer (ref. 20, 31), since

191 recent studies suggest that EMPD and mammary Paget's disease (a breast cancer)

192 harbor common recurrent mutations (ref 24, 32). The eribulin administration showed

193 high efficacy against all of EMPD-PDX-H1 tumors. Although there are no clinical

194 reports of eribulin being effective against EMPD-PDX-H1, it is suggested that eribulin

195 may be a treatment option for EMPD.

196   Unfortunately, we established the EMPD-PDX from only one patient in the

197   present study due to the small number of advanced EMPD cases. In the future, it is

198   necessary to confirm whether PDX models can be established from other patients using

199   the same methods and to conduct treatment experiments on other PDX models to

200   develop preclinical studies. Despite this limitation, EMPD-PDX-H1 is the first to

201   investigate the efficacy of antitumor agents and to help in the search for new treatments

202   for advanced EMPD.

203   In summary, we generated a novel EMPD PDX model that maintained the

204   original patient's tumors both histopathologically and genetically. Our therapeutic

205   experiments revealed *in vivo* tumor growth inhibition by anti-HER2 therapies (lapatinib

206   and trastuzumab) and cytotoxic agents (docetaxel and eribulin). EMPD-PDX-H1 could

207   be useful for developing effective therapies for EMPD.

208

209 **Materials and Methods**

210 **Samples from the EMPD patient**

211 EMPD tissues were obtained from inguinal lymph node metastases of a 78-year-old

212 Japanese female whose primary genital skin lesion had been removed 12 years before

213 the lymph node metastasis occurred (Figure 2 A, B). She had no significant familial or

214 past medical history. The resected metastatic lymph node was separated into two parts:

215 One was immediately transported on ice for transplantation, and the other was fixed in

216 formalin and embedded into paraffin for pathological diagnosis. Written informed

217 consent was obtained from the patient, and this research was approved by the Ethics

218 Committee of Hokkaido University Hospital in accordance with the Declaration of

219 Helsinki (IRB approval number: 018-0424).

220

221 **Establishment of EMPD-PDX-H1**

222 A 10-mm-wide piece of EMPD tissue was subcutaneously transplanted with Matrigel

223 (BD Bioscience, Franklin Lakes, NJ, USA) onto both flanks of a 5-week-old female

224 NOD/Scid mouse (Clea, Tokyo, Japan). The mice in this study were housed in a specific

225 pathogen-free condition at a fixed temperature (22–25°C) and were held on a 12-hour

226 light-dark cycle. The mice were given distilled water and standard chow *ad libitum*.

227 Animal use procedures were approved by the institutional committee of Hokkaido

228   University (approval numbers 19-0015 and 19-0093). The tumor-transplanted mouse

229   was observed twice a week for 5 months. The tumors were measured once a week by

230   caliper. Tumor volume was calculated using the following formula: (long axis x short

231   axis^2)/2 (ref. 33). Once the tumor volume reached 500–1000 mm^3, EMPD-PDX-H1

232   tumors were transplanted into the next generation of NOD/Scid mice. In the first two

233   consecutive mouse-to-mouse passages, EMPD-PDX-H1 tumors were separated into

234   three sections: The first part was cut into pieces (less than 5 mm in diameter) for

235   transplantation, and the second part was frozen immediately at −80 °C for DNA

236   extraction and was fixed in formalin and then embedded into paraffin for pathological

237   analysis. Treatment experiments were performed on the 3rd–5th generations. At the 4th

238   passage, transplantation was also performed on 5-week-old female nude (*nu/nu*) mice

239   (Clea, Tokyo, Japan). Greater amounts of fresh tumor pieces at passages 4 and 5 were

240   frozen in CryoStor® CS10 (BioLife Solutions, Owego, NY, USA) and stored at −80 °C

241   (ref. 34). The cryopreserved EMPD-PDX-H1 tumors were re-transplanted into

242   NOD/Scid mice to confirm reanimation.

243

244   **Histopathological analyses**

245   Formalin-fixed, paraffin-embedded tissue sections of the patient's tumors or the

246   xenografted tumors were cut into 4-µm sections. Hematoxylin and eosin (HE) staining

14

247   as well as immunohistochemistry for CK7 (Dako, Code. M7018, Denmark), HER2

248   (Dako, Code. A0485, Denmark), androgen receptor (ScyTek laboratories, RA0012-C,

249   USA), estrogen receptor (Leica Biosystems, NCL-L-6F11, UK), progesterone receptor

250   (Leica Biosystems, NCL-L-PGR-312, UK) and Ki-67 (Abcam, #ab8191) were

251   performed to compare the histopathology of the primary lesions, metastatic lymph

252   nodes, and xenografts. DAB chromogen was applied to yield a brown color (ref. 35).

253   For nuclear Ki-67 expression, the percentage of positive cells among at least 100 cancer

254   cells from three randomly selected fields of vision using a high-power lens (x 400) were

255   calculated. The expression levels of HER2 protein were evaluated according to the

256   HER2 testing guideline for breast cancer as follows (ref. 36).

257   3+: "circumferential membrane staining that is complete, intense"

258   2+: "circumferential membrane staining that is incomplete and/or weak to moderate and

259   within > 10% of the invasive tumor cells or complete and circumferential membrane

260   staining that is intense and within ≤ 10% of the invasive tumor cells"

261   1+: "incomplete membrane staining that is faint or barely perceptible and within > 10%

262   of the invasive tumor cells"

263   0: "no staining observed or membrane staining that is incomplete and is faint or barely

264   perceptible and within ≤ 10% of the invasive tumor cells"

265

266 **TUNEL assays**

267 Cell death was assessed by the TUNEL method using an In Situ Cell Death Detection

268 Kit (Roche, #11684817910) according to the manufacturer's instructions. For nuclear

269 TUNEL staining, the percentage of positive cells among at least 100 cancer cells from

270 three randomly selected fields of vision using a high-power lens (x 400) was calculated.

271

272 **Gene mutation analysis**

273 EMPD patient tissues and EMPD-PDX-H1 tissues were pathologically reviewed to

274 ensure that the tumor cell content was high enough and that no significant tumor

275 necrosis had occurred before DNA extraction. Genomic DNA was extracted from our

276 patient's blood and from each tissue sample using the DNA Mini Kit (QIAGEN,

277 Cat#51304, Germany) or the GeneRead FFPE DNA Kit (QIAGEN, Cat#180134,

278 Germany). The quantity and purity of DNA samples were measured using a Nanodrop

279 ND-1000 UV/VIS Spectrophotometer (Thermo Scientific, USA). DNA fragment

280 integrity was confirmed by electrophoresis using 1% agarose gel. The concentrations of

281 DNA samples were normalized to 20 ng/μl, and those samples were stored at −20°C

282 until use. Genomic testing was performed at the genomic unit of the Keio Cancer Center

283 in Tokyo, Japan. After the quality of the DNA was checked based on the DNA integrity

284 number (DIN) score calculated using the Agilent 2000 TapeStation (Agilent

16

285   Technologies, Waldbronn, Germany), targeted amplicon exome sequencing for 160

286   cancer-related genes was performed using the Illumina MiSeq sequencing platform

287   (Illumina, San Diego, CA). The list of 160 cancer-related genes included in the

288   comprehensive cancer panel is shown in Supplementary Table S2. The minimum

289   amount of DNA was 50 ng, and the minimum quality for DNA was that with a DIN

290   score over 3.1. The sequencing data were analyzed using an original bioinformatics

291   pipeline called GenomeJack (Mitsubishi Space Software, Tokyo, Japan). In addition, we

292   performed mutation analysis by Sanger sequencing to confirm the pathogenic *ERBB2*

293   gene alteration in the primary lesions using the following primers: forward primer 5'-

294   CGGTAATGCTGCTCATGGTG-3' and reverse primer 5'-

295   CTTGCTGCACTTCTCACACC-3'.

296

297   **EMPD-PDX-H1-derived primary cell culture**

298   Tumor tissue from EMPD-PDX-H1 mice (3rd generation) was minced and washed with

299   PBS repeatedly. The minced tissue was directly plated onto dishes coated with type I

300   collagen (Iwaki, Tokyo, Japan) in a medium of RPMI (Nakalai, Kyoto, Japan)

301   containing 10% fetal bovine serum (FBS, Sigma).

302

303   **Treatment experiments using EMPD-PDX-H1**

17

304 Tumor growth curves for all EMPD-PDX-H1 were generated using the kinetic

305 measurement of tumor volumes. The tumor volume range of 50 to 100 mm^3 in the

306 tumor-bearing NOD/Scid mice was randomized, and treatment experiments were begun.

307 All treatment experiments were performed with a minimum of n = 4 mice per condition.

308 Control mice were administered with 100 μl of 0.5% hydroxypropyl methylcellulose

309 once a day orally (n = 5), intraperitoneally injected with 100 μl of PBS twice per week

310 (n = 5), or intravenously injected with 100 μl of PBS once per week (n = 5). In the

311 HER2-targeted treatments, trastuzumab (10 mg/kg, Herceptin®, Chugai Pharmaceutical

312 Co., Ltd., Tokyo, Japan) was given intraperitoneally twice weekly according to a

313 previous study (ref. 37). Lapatinib (100 mg/kg, CS-0036, Chem Scene, USA) was

314 administered once a day orally in 0.5% hydroxypropyl methylcellulose and 0.1% Tween

315 80 (P1754, Sigma-Aldrich, Germany) (ref. 38). We also administered trastuzumab and

316 lapatinib in combination (ref. 37). Concerning cytotoxic agents, docetaxel (20 mg/kg,

317 Santa Cruz Biotechnology, CA, USA, #sc-201436) and eribulin (1.5 or 0.45 mg/kg,

318 Halaven, Eisai Co., Ltd., Tokyo, Japan) were administered intravenously once per week

319 (ref. 31, 39). Tumor volumes were measured once a week by caliper, and tumor weights

320 were measured with a scale at 28 days after treatment initiation. Tumor volume and

321 weight were recorded in a blinded manner.

322

18

323   **Statistical analysis**

324   To evaluate the statistical significance of the treatment experiments, Student's *t*-test was

325   used to compare tumor volume between the treatment groups and the control group.

326   Statistical tests were two sided, with $P < 0.05$ considered significant.

327

328 **Disclosure of Potential Conflicts of Interest**

329 None to declare.

330

331 **Acknowledgments**

335

336   **References**

337   1.   Paget SJ. On disease of the mammary areola preceding cancer of the mammary

338   gland. St. Bartholomew's Hosp Rep. 1874; 10:87–9.

339   2.   Kanitakis J. Mammary and extramammary Paget's disease. J Eur Acad

340   Dermatol Venereol. 2007; 21:581–90.

341   3.   Herrel LA, Weiss AD, Goodman M, Johnson TV, Osunkoya AO, Delman KA,

342   et al. Extramammary Paget's disease in males: survival outcomes in 495

343   patients. Ann Surg Oncol. 2015; 22:1625–30.

344   4.   Karam A, Dorigo O. Treatment outcomes in a large cohort of patients with

345   invasive Extramammary Paget's disease. Gynecol Oncol. 2012; 125:346–51.

346   5.   Hatta N, Yamada M, Hirano T, Fujimoto A, Morita R. Extramammary Paget's

347   disease: treatment, prognostic factors and outcome in 76 patients. Br J

348   Dermatol. 2008; 158:313–8.

349   6.   Hirakawa S, Detmar M, Kerjaschki D, Nagamatsu S, Matsuo K, Tanemura A,

350   et al. Nodal lymphangiogenesis and metastasis: Role of tumor-induced

351   lymphatic vessel activation in extramammary Paget's disease. Am J Pathol.

352   2009; 175:2235–48.

353   7.   Ohara K, Fujisawa Y, Yoshino K, Kiyohara Y, Kadono T, Murata Y, et al. A

354   proposal for a TNM staging system for extramammary Paget disease:

21

355   Retrospective analysis of 301 patients with invasive primary tumors. J

356   Dermatol Sci. 2016 Sep;83(3):234–9.

357   8.   Oashi K, Tsutsumida A, Namikawa K, Tanaka R, Omata W, Yamamoto Y, et al.

358   Combination chemotherapy for metastatic extramammary Paget disease. Br J

359   Dermatol. 2014; 170:1354–7.

360   9.   Tokuda Y, Arakura F, Uhara H. Combination chemotherapy of low-dose 5-

361   fluorouracil and cisplatin for advanced extramammary Paget's disease. Int J

362   Clin Oncol. 2015; 20:194–7.

363   10.   Yoshino K, Fujisawa Y, Kiyohara Y, Kadono T, Murata Y, Uhara H, et al.

364   Usefulness of docetaxel as first-line chemotherapy for metastatic

365   extramammary Paget's disease. J Dermatol. 2016; 43:633–7.

366   11.   Kato M, Yoshino K, Maeda T, Nagai K, Oaku S, Hiura A, et al. Single-agent

367   taxane is useful in palliative chemotherapy for advanced extramammary

368   Paget's disease; A Case Series. Br J Dermatol. 2019; 181:831–2.

369   12.   Hirai I, Tanese K, Nakamura Y, Ishii M, Kawakami Y, Funakoshi T.

370   Combination Cisplatin-Epirubicin-Paclitaxel Therapy for Metastatic

371   Extramammary Paget's Disease. Oncologist. 2019; 24:e394–6.

372   13.   Karam A, Berek JS, Stenson A, Rao J, Dorigo O. HER-2/neu targeting for

373   recurrent vulvar Paget's disease: a case report and literature review. Gynecol

374   Oncol. 2008; 111:568–71.

375   14.   Takahagi S, Noda H, Kamegashira A, et al. Metastatic extramammary Paget's

376   disease treated with paclitaxel and trastuzumab combination chemotherapy. J

377   Dermatol. 2009 36:457–61.

378   15.   Vornicova O, Hershkovitz D, Yablonski-Peretz T, Ben-Itzhak O, Keidar Z, Bar-

379   Sela G. Treatment of metastatic extramammary Paget's disease associated with

380   adnexal adenocarcinoma, with anti-HER2 drugs based on genomic alteration

381   ERBB2 S310F. Oncologist. 2014; 19:1006–7.

382   16.   Bertotti A, Migliardi G, Galimi F, Sassi F, Torti D, Isella C, et al. A molecularly

383   annotated platform of patient-derived xenografts ("xenopatients") identifies

384   HER2 as an effective therapeutic target in cetuximab-resistant colorectal

385   cancer. Cancer Discov. 2011; 1:508–23.

386   17.   Hidalgo M, Amant F, Biankin AV, Budinská E, Byrne AT, Caldas C, et al.

387   Patient-derived xenograft models: an emerging platform for translational

388   cancer research. Cancer Discov. 2014; 4:998–1013.

389   18.   Koga Y, Ochiai A. Systematic Review of Patient-Derived Xenograft Models for

390   Preclinical Studies of Anti-Cancer Drugs in Solid Tumors. Cells. 2019; 8:E418.

391   19.   Nishi M, Tashiro M, Yoshida H. Stimulation of growth by both androgen and

392   estrogen of the EMP-K1 transplantable tumor with androgen and estrogen

393   receptors from human extramammary Paget's disease in nude mice. J Natl

394   Cancer Inst. 1992; 84:519–23.

395   20.   Twelves C, Cortes J, Vahdat L, Olivo M, He Y, Kaufman PA, et al. Efficacy of

396   eribulin in women with metastatic breast cancer: a pooled analysis of two

397   phase 3 studies. Breast Cancer Res Treat. 2014; 148:553–61.

398   21.   Richter CE, Hui P, Buza N, Silasi DA, Azodi M, Santin AD, et al. HER-2/NEU

399   overexpression in vulvar Paget disease: the Yale experience. J Clin Pathol.

400   2010; 63:544–7.

401   22.   Tanaka R, Sasajima Y, Tsuda H, Namikawa K, Tsutsumida A, Otsuka F, et al.

402   Human epidermal growth factor receptor 2 protein overexpression and gene

403   amplification in extramammary Paget disease. Br J Dermatol. 2013; 168:1259–

404   66.

405   23.   Tanaka R, Sasajima Y, Tsuda H, Namikawa K, Takahashi A, Tsutsumida A, et

406   al. Concordance of the HER2 protein and gene status between primary and

407   corresponding lymph node metastatic sites of extramammary Paget disease.

408   Clin Exp Metastasis. 2016; 33:687–97.

409   24.   Zhang G, Zhou S, Zhong W, Hong L, Wang Y, Lu S, et al. Whole-Exome

410   Sequencing Reveals Frequent Mutations in Chromatin Remodeling Genes in

411   Mammary and Extramammary Paget's Diseases. J Invest Dermatol. 2019;

412   139:789–795.

413   25.   Kiniwa Y, Yasuda J, Saito S, Saito R, Motoike IN, Danjoh I, et al. Identification

414   of genetic alterations in extramammary Paget disease using whole exome

415   analysis. J Dermatol Sci. 2019; 94:229–235.

416   26.   Tate JG, Bamford S, Jubb HC, Sondka Z, Beare DM, Bindal N, et al.

417   COSMIC: the Catalogue Of Somatic Mutations In Cancer. Nucleic Acids Res.

418   2019; 47:D941–7.

419   27.   Greulich H, Kaplan B, Mertins P, Chen TH, Tanaka KE, Yun SH, et al.

420   Functional analysis of receptor tyrosine kinase mutations in lung cancer

421   identifies oncogenic extracellular domain mutations of ERBB2. Proc Natl Acad

422   Sci U S A. 2012; 109:14476–81.

423   28.   Ma CX, Bose R, Gao F, Freedman RA, Telli ML, Kimmick G, et al. Neratinib

424   Efficacy and Circulating Tumor DNA Detection of HER2 Mutations in HER2

425   Nonamplified Metastatic Breast Cancer. Clin Cancer Res. 2017; 23:5687–95.

426   29.   Kavuri SM, Jain N, Galimi F, Cottino F, Leto SM, Migliardi G, et al. HER2

427   activating mutations are targets for colorectal cancer treatment. Cancer Discov.

428   2015; 5:832–41.

429   30.   Hyman DM, Piha-Paul SA, Won H, Won H, Rodon J, Saura C, et al. HER

430   kinase inhibition in patients with HER2- and HER3-mutant cancers. Nature.

431   2018; 554:189–194.

432   31.   Towle MJ, Nomoto K, Asano M, Kishi Y, Yu MJ, Littlefield BA. Broad

433   spectrum preclinical antitumor activity of eribulin (Halaven(R)): optimal

434   effectiveness under intermittent dosing conditions. Anticancer Res. 2012;

435   32:1611–9.

436   32.   Takeichi T, Okuno Y, Matsumoto T, Tsunoda N, Suzuki K, Tanahashi K, et al.

437   Frequent FOXA1-Activating Mutations in Extramammary Paget's Disease.

438   Cancers (Basel). 2020; 12(4).

439   33.   Yanagi T, Krajewska M, Matsuzawa S, Reed JC. PCTAIRE1 phosphorylates

440   p27 and regulates mitosis in cancer cells. Cancer Res 2014; 74:5795–807.

441   34.   Ivanics T, Bergquist JR, Liu G, Kim MP, Kang Y, Katz MH, et al. Patient-

442   derived xenograft cryopreservation and reanimation outcomes are dependent on

443   cryoprotectant type. Lab Invest. 2018; 98:947–956.

444   35.   Yanagi T, Watanabe M, Hata H, Kitamura S, Imafuku K, Yanagi H, et al. Loss

445   of TRIM29 Alters Keratin Distribution to Promote Cell Invasion in Squamous

446   Cell Carcinoma. Cancer Res. 2018; 78:6795-6806.

447   36.   Wolff AC, Hammond MEH, Allison KH, Harvey BE, Mangu PB, Bartlett JMS,

448   et al. Human Epidermal Growth Factor Receptor 2 Testing in Breast Cancer:

449   American Society of Clinical Oncology/College of American Pathologists

450   Clinical Practice Guideline Focused Update. J Clin Oncol. 2018; 36: 2105–22.

451   37.   Wainberg ZA, Anghel A, Desai AJ, Ayala R, Luo T, Safran B, et al. Lapatinib, a

452   dual EGFR and HER2 kinase inhibitor, selectively inhibits HER2-amplified

453   human gastric cancer cells and is synergistic with trastuzumab in vitro and in

454   vivo. Clin Cancer Res. 2010; 16:1509–19.

455   38.   Nonagase Y, Yonesaka K, Kawakami H, Watanabe S, Haratani K, Takahama T,

456   et al. Heregulin-expressing HER2-positive breast and gastric cancer exhibited

457   heterogeneous susceptibility to the anti-HER2 agents lapatinib, trastuzumab

458   and T-DM1. Oncotarget. 2016; 7:84860–71.

459   39.   Hendrikx JJ, Lagas JS, Song JY, Rosing H, Schellens JHM, Beijnen JH, et al.

460   Ritonavir inhibits intratumoral docetaxel metabolism and enhances docetaxel

461   antitumor activity in an immunocompetent mouse breast cancer model. Int J

462   Cancer. 2016; 138:758–69.

463

464   **Figure legends**

465   **Figure 1. Schematic of the study method**

466   Tissue obtained from the EMPD patient is transplanted into NOD/Scid mice (generation

467   0: G0). The xenografted tumors are transplanted to further generations (G1-G4) and

468   used for cell culture, histopathological analysis, genetic analysis, and treatment

469   experiments.

470

471   **Figure 2. The clinical manifestations and immunohistopathological findings for the**

472   **primary site, the metastatic lymph node, and EMPD-PDX-H1**

473   A, Clinical photo of the patient's primary tumor. B, Computed tomography image of the

474   patient's lymph node metastasis (yellow arrow) and the clinical photo (inset). C,

475   Appearance of the xenografted tumor on a NOD/Scid mouse (red arrowheads). D,

476   Hematoxylin and eosin staining and immunohistochemistry of CK7 and HER2. The

477   score for HER2 expression in invasive tumor cells was 1+, which is consistent with that

478   in PDX tissue. Scale bar = 100 μm.

479
480   **Figure 3. EMPD-PDX-H1 tumors harbor *ERBB2* gene mutations identical to those**

481   **of the patient's primary and metastatic tumors.**

482   A, Actionable genetic alterations in the patient's samples and EMPD-PDX-H1 tumors

483   through deep sequencing using a comprehensive cancer panel. Identical gene alterations

484   (*ERBB2* p.S310F) are detected in original patient's tumor samples (lymph node

485   metastasis: LN), PDX (G1), and PDX (G2). B, Sanger sequencing results. An identical

486   *ERBB2* mutation is detected in the patient's primary tumor.

487

488   **Figure 4. HER2-targeted therapies suppress the tumor growth of EMPD-PDX-H1**

489   **harboring the *ERBB2* S310F mutation.**

490   Tumor-bearing NOD/Scid mice were randomized into no therapy, lapatinib 100

491   mg/kg/day orally (A, B), trastuzumab 10 mg/kg intraperitoneally twice a week (C, D),

492   or a combination of these two agents (E, F). Green arrowheads indicate the injection of

493   trastuzumab. Tumor volumes and weights were calculated and analyzed as indicated in

494   Materials and Method. The results are presented as means, with the error bars

495   representing the SD from the mean. All comparisons were statistically significant

496   between the following groups: combo, trastuzumab or lapatinib versus no therapy.

497

498   **Figure 5. EMPD-PDX-H1 are sensitive to cytotoxic agents, including eribulin and**

499   **docetaxel.**

500   Treatment experiments of cytotoxic agents using EMPD-PDX-H1. Tumor-bearing

501   NOD/Scid mice were randomly treated with one of following injections: docetaxel at 20

502   mg/kg once a week (A, B), eribulin at 1.5 mg/kg once a week (C, D), eribulin at 0.45

503   mg/kg (E, F) or sterile PBS once a week (control). The results are presented as means,

504   with the error bars representing the SD from the mean. All comparisons are statistically

505   significant between the following groups: the docetaxel group or the eribulin groups

506   versus the control, $P < 0.001$. Blue, green, and red arrowheads indicate the injection of

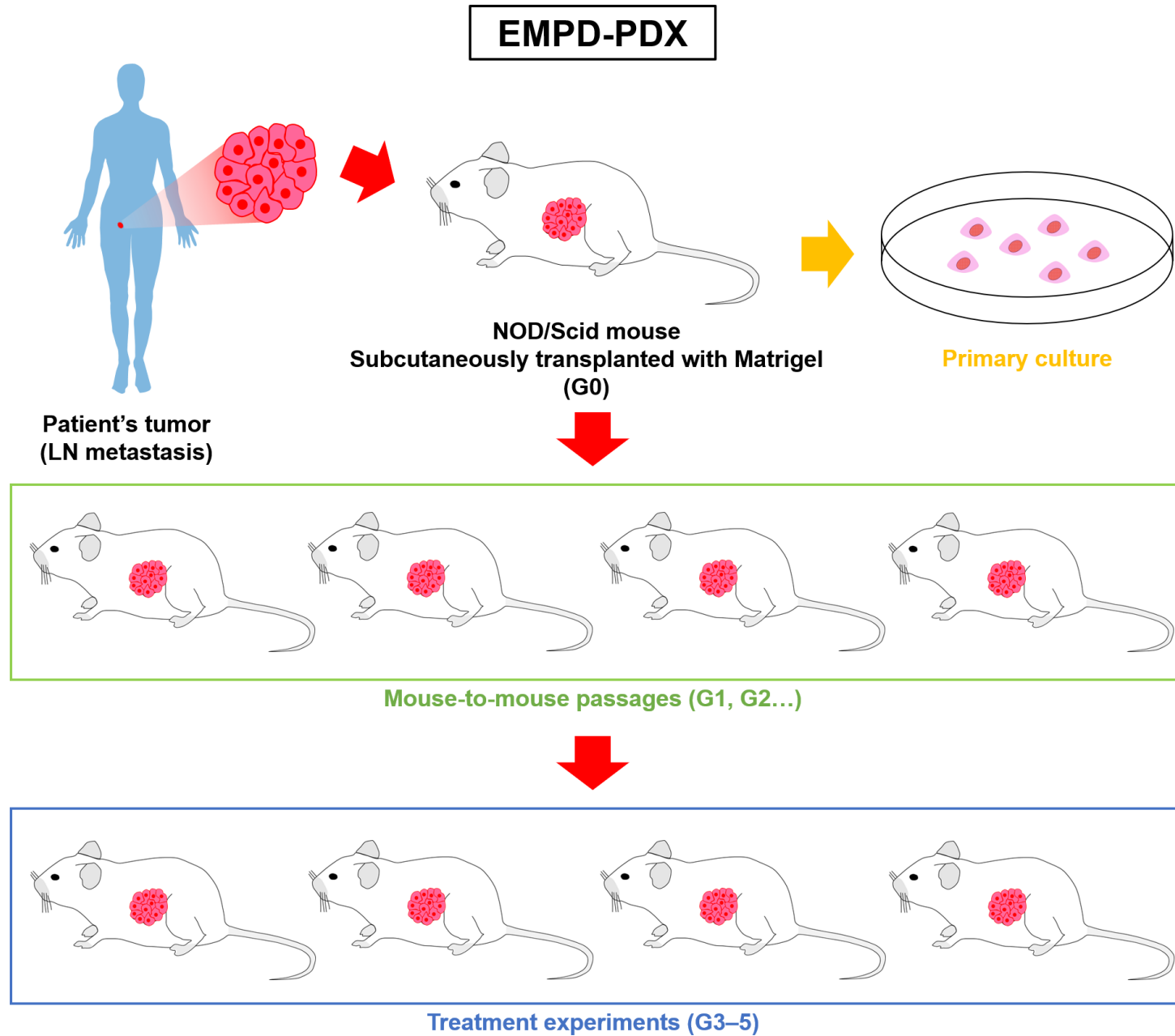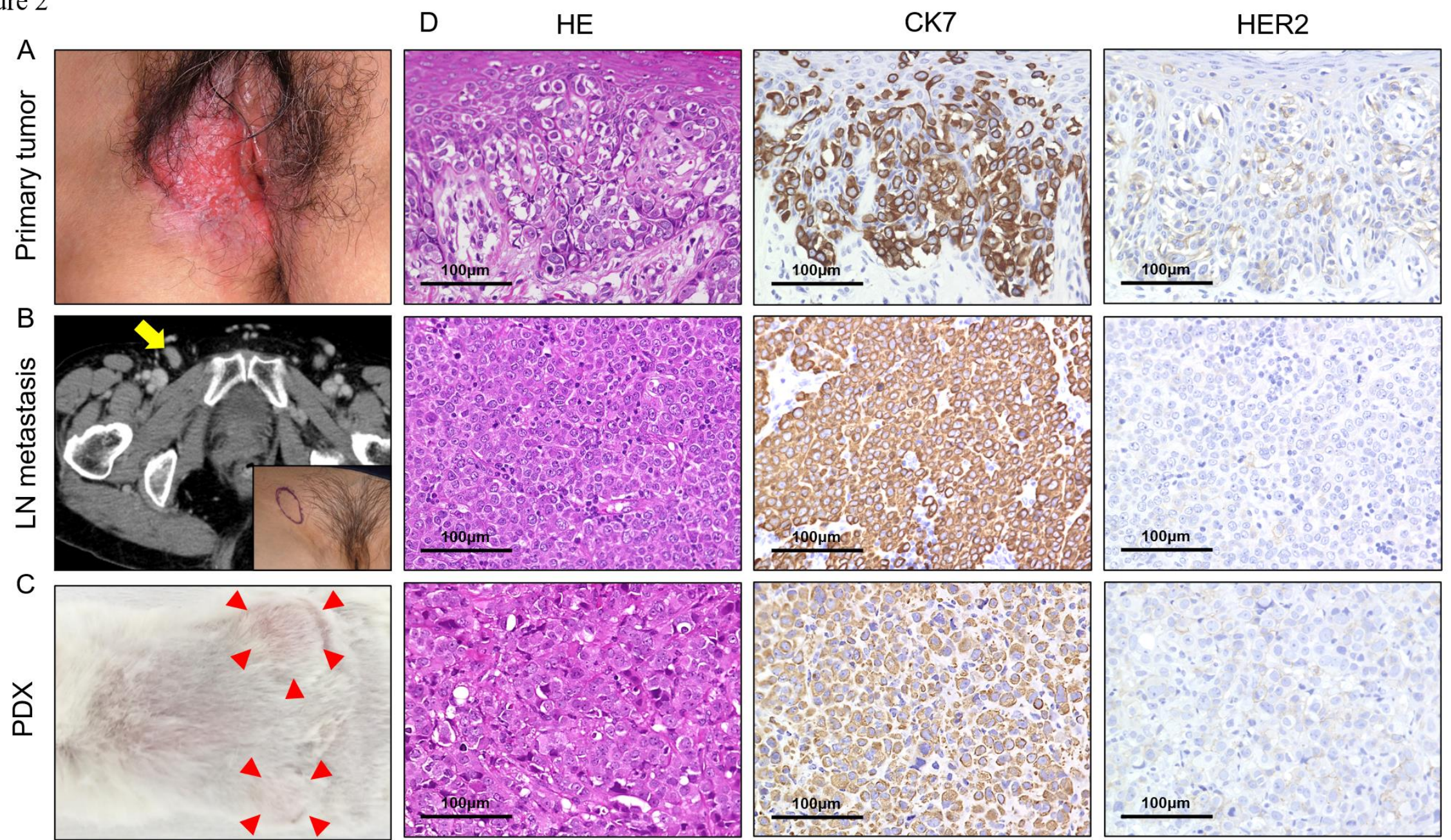507   docetaxel, eribulin 1.5 mg/kg or eribulin at 0.45 mg/kg, respectively.

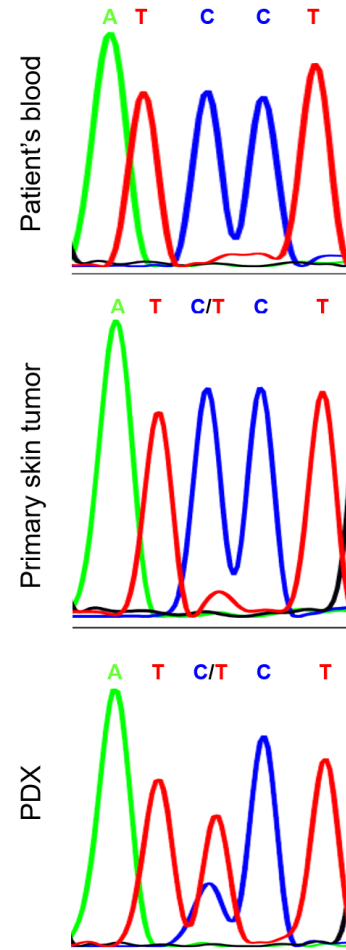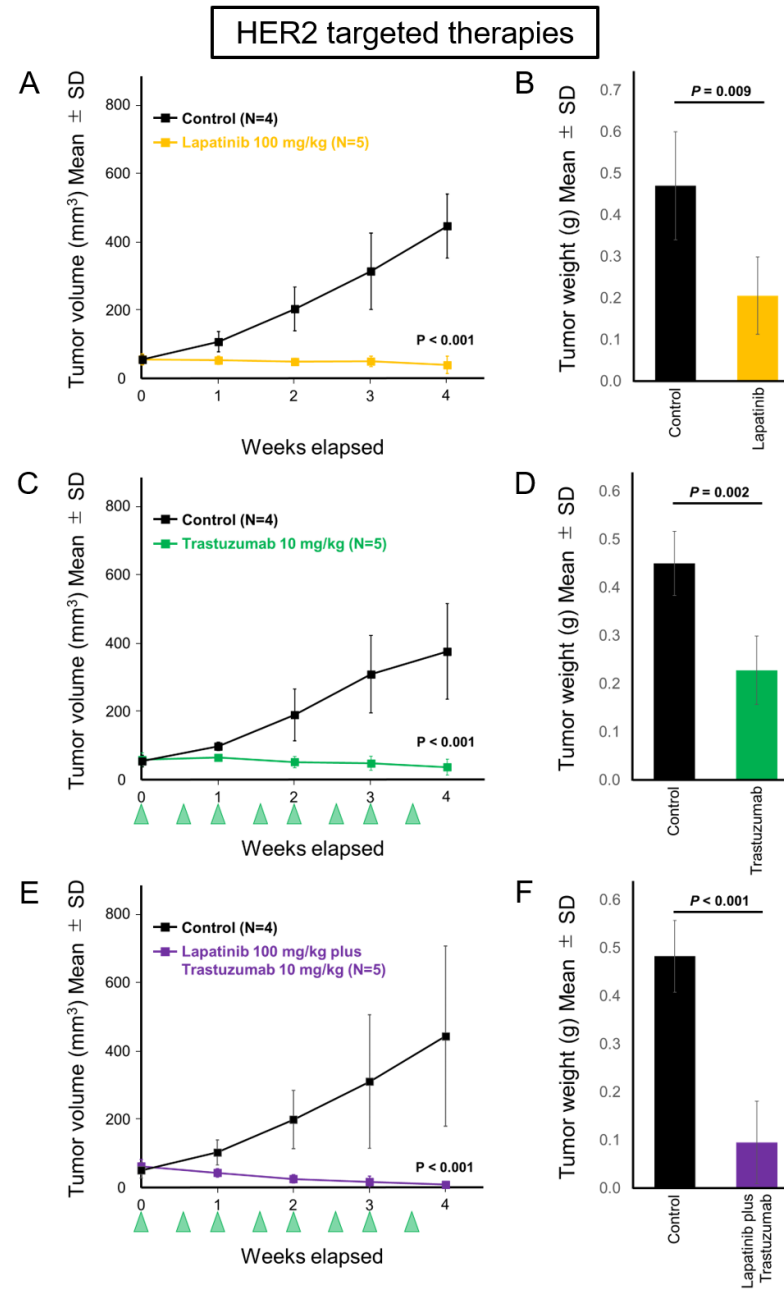**EMPD-PDX**

Patient's tumor
(LN metastasis)

NOD/Scid mouse
Subcutaneously transplanted with Matrigel
(G0)

Primary culture

Mouse-to-mouse passages (G1, G2…)

Treatment experiments (G3–5)

Maeda et al.
Figure 3

A

Sample characteristics	Major gene alterations (VAF, %)
Patient's blood	None
Patient's LN	*ERBB2* S310F (51.6%)
PDX (G1)	*ERBB2* S310F (70.7%)
PDX (G2)	*ERBB2* S310F (68.5%)

VAF: variant allele frequency

B **ERBB2 S310F (c.929C>T)**

HER2 targeted therapies

Cytotoxic chemotherapies